Complex Coordinates in Near Hovering Rotor Dynamics

H. C. Curtiss Jr.*
Princeton University, Princeton, N. J.

The application of complex coordinates to the study of the dynamic characteristics of the tip-path-plane of a helicopter rotor is considered. The coordinates describing rotor blade motions can be transformed from individual blade flapping angles to linear combinations of flapping angles. Two of the transformed coordinates can be interpreted as describing the tilting motion of the tip-path-plane. In a stationary reference frame, these two new coordinates are coupled. However, by defining a set of complex coordinates, for near hovering flight these two coupled differential equations can be combined into a single second-order differential equation describing the tilting motion of the tip-path-plane. This formulation provides a convenient and natural framework for investigation of the response characteristics of fully articulated and hingeless rotors. Considerable insight into the influence of various physical parameters on the behavior of the tip-path-plane can be gained. The approach is illustrated by consideration of the transient and frequency response characteristics of the tip-path-plane and the influence of flapping feedback. An extension of the root locus method is described which makes the investigation of flapping feedback convenient.

Nomenclature†

a = rotor blade lift curve slope
b = number of blades
$A(s)$ = transfer function
c = rotor blade chord
C_l = rotor hub rolling moment coefficient, positive for right roll, $C_l = \mathrm{L}/\rho\pi R^2(\Omega R)^2R$
C_m = rotor hub pitching moment coefficient, positive nose up, $C_m = M/\rho\pi R^2(\Omega R)^2R$
C_{mz} = complex rotor hub moment coefficient, $C_{mz} = C_m + iC_l$
I_1 = rotor blade flapping moment of inertia
j = constant of proportionality between complex inflow and complex rotor aerodynamic hub moment coefficient
K_H = gain parameter associated with integral flapping feedback
K_P, K_ϵ = parameters associated with proportional flapping feedback
m_z = dimensionless aerodynamic moment acting on rotor blade due to forward speed. Effect of cyclic pitch, angular rates and flapping not included
p = rotor blade natural frequency in flapping divided by rotor rpm, also roll rate nondimensionalized by rotor rpm, positive roll right
q = pitch rate nondimensionalized by rotor rpm, positive nose up
R = rotor blade radius
s = Laplace operator, nondimensionalized by rotor rpm
V = flight velocity
α = dimensionless blade stiffness parameter, $\alpha = (p^2 - 1)/\eta$
α^* = blade stiffness parameter, modified to account for first harmonic inflow, $\alpha^* = [1 + (4/3)j]\alpha$
β_i = flapping angle of ith blade, positive for upward flapping
γ = Lock number, $\gamma = \rho acR^4/I_1$
Δ_c = complex coordinate, cyclic pitch, $\Delta_c = A_1 + iB_1$
$\Delta\lambda$ = complex first harmonic inflow, positive up, $\Delta\lambda = \lambda_c + i\lambda_s$
δ = complex coordinate, tilting of tip-path-plane in stationary coordinate system, $\delta = a_1 + ib_1$
Σ = complex coordinate, tilting of tip-path-plane in rotating coordinate system, $\Sigma = \sigma_1 + i\sigma_2$
η = dimensionless parameter, $\eta = \gamma/8$
η^* = dimensionless parameter, modified to account for first harmonic inflow, $\eta^* = \eta/[1 + (4/3)j]$
ρ = air density
μ = advance ratio, $V/\Omega R$
ν = complex coordinate, angular rate of rotation of shaft divided by rotor rpm, $\nu = q + ip$
Ω = rotor blade angular velocity
σ = real part of characteristic root, nondimensionalized by rotor rpm; also rotor solidity, $bc/\pi R$
σ_0 = coning, $\sigma_0 = \frac{1}{4}(\beta_1 + \beta_2 + \beta_3 + \beta_4)$
σ_1 = tip-path-plane tilting coordinate in rotating system, $\sigma_1 = \frac{1}{2}(\beta_1 - \beta_3)$
σ_2 = tip-path-plane tilting coordinate in rotating system, $\sigma_2 = \frac{1}{2}(\beta_2 - \beta_4)$
σ_3 = differential collective flapping, $\frac{1}{4}(\beta_1 + \beta_3 - \beta_2 - \beta_4)$
τ = time nondimensionalized by rotor rpm
ψ_i = azimuth angle of ith blade, referenced to downwind
ω = natural frequency or forcing frequency nondimensionalized by rotor rpm
$(\dot{}), (\ddot{})$ = differentiation with respect to time nondimensionalized by rotor rpm
$(\,)_{ss}$ = steady-state value

Introduction

IN recent years increased interest and importance has been placed on rotor blade dynamics, particularly with the introduction of hingeless rotors.[1,2]

The fully articulated rotor has been in existence for a number of years and the effects of various physical parameters on its behavior are reasonably well understood. It becomes more difficult to understand the manner in which the various rotor parameters and the flight condition influence rotor blade flapping behavior when hingeless rotors of various stiffness are considered. This paper develops a method which is convenient for examining the response characteristics of rotor blades such that the interactions of the various physical parameters of the rotor in influencing the response can be clearly seen. It is particularly suited to studies near hovering flight and loses its simplicity as the advance ratio increases. However, other complications also enter the dynamic analysis of rotor blade motion at high advance ratios such that closed

Presented as Paper 72-954, at the AIAA 2nd Atmospheric Flight Mechanics Conference, Palo Alto, Calif., September 11-13, 1972; submitted October 31, 1973; revision received March 21, 1973.

Index categories: Rotary Wing Aerodynamics; VTOL Handling, Stability and Control.

*Professor, Department of Aerospace and Mechanical Sciences. Member AIAA.

†The cyclic pitch applied to the rotor blade 1 is $-A_1\cos\psi_1 - B_1\sin\psi_1$ and the harmonic inflow experienced by rotor blade 1 is $\lambda_c\cos\psi_1 + \lambda_s\sin\psi_1$.

form solutions are not possible.[3] No particular attempt is made to discuss specific rotor problems but rather the approach is illustrated by various examples pertinent to problems of current interest.

Hohenemser in recent papers[1,4] has clarified the concept of the rotor tip-path-plane in a dynamic situation by defining multiblade coordinates. He notes that a similar approach was used by Coleman in the study of ground resonance.[5] Coleman also introduced the concept of complex displacements and it is this approach which will be followed as a natural way to describe the tip-path-plane motion of a rotor. Some examples of this approach with respect to flapping dynamics are found in the literature,[6,7] however, the approach has not been fully developed to show the simplicity and insight which can be gained in the study of the flapping motion of a rotor. Although the formulation presented can be used at higher speeds, its simplicity depends upon a certain symmetry inherent in the equations for flapping motion which is lost as the μ^2 terms become significant. However, the coefficients in the equations also have periodic terms which depend upon μ^2 and one must turn to machine methods for response calculations as these terms become significant. Therefore, the analysis presented is restricted to low advance ratio conditions. An extension of the root locus method will be described which makes the study of various flapping feedback systems convenient.

An additional feature of the approach is the simplicity of conversion from moving to stationary coordinates, and the interpretation of progressive and regressive modes follows directly from the mathematical formulation.

Analysis

It will be assumed that the flapping motion of the blades can be described by linearized small perturbation equations, and that the flapping motion and hub moment characteristics of a hingeless rotor blade can be represented by a rigid blade with a spring on the flapping hinge. The latter assumption is made for simplicity. It has been shown that care should be taken with this approximation when investigating hingeless rotors.[8] For simplicity, the analysis is presented for a four-bladed rotor, however, the results relating to tilting of the tip-path-plane are not affected by the number of blades.

The coordinates describing the flapping motion of each rotor blade are combined in linear combinations, equivalent to Hohenemser's multiblade coordinates to form four new coordinates in the case of a four-bladed rotor. One of these coordinates can be interpreted as the coning angle, two are associated with tilting of the tip-path-plane, and one is associated with a differential collective flapping of the tip-path-plane. The interest here centers on the coordinates describing the tilting motion only. The two coordinates describing the tilting of tip-path-plane are combined to form a single coordinate. In fact, two new coordinates are defined, the complex coordinate to be treated and its conjugate. For the assumed flight conditions of interest near hovering, the equation of motion for the conjugate variable is uncoupled and a simpler formulation for the tip-path-plane dynamics results. At higher speeds, the complex variable and its conjugate will be dynamically coupled. The approach used is still valid, however it loses its simplicity.

The linearized flapping equation for the ith blade may be written as[4]

$$\ddot{\beta}_i + (\frac{\gamma}{8} + \frac{\gamma\mu}{6}\sin\psi_i)\dot{\beta}_i + (p^2 + \frac{\gamma\mu}{6}\cos\psi_i)\beta_i = A + B\cos\psi_i + C\sin\psi_i \quad (1)$$

where A, B and C are dependent upon control inputs and the flight condition of the rotor. Reverse flow and terms dependent upon μ^2 are neglected since near hovering flight is of interest.

Numbering the blades in the direction of rotation and defining a new set of coordinates:

$$\sigma_0 = \frac{\beta_1 + \beta_2 + \beta_3 + \beta_4}{4} \qquad \sigma_2 = \frac{\beta_2 - \beta_4}{2}$$

$$\sigma_1 = \frac{\beta_1 - \beta_3}{2} \qquad \sigma_3 = \frac{(\beta_1 + \beta_3) - (\beta_2 + \beta_4)}{4}$$

These coordinates are multiblade coordinates[4] defined for a four-bladed rotor in a reference frame rotating with the rotor blades. Equations (1) for the individual blade motions are combined to obtain four new equations of motion in terms of these variables. Then the equation for σ_2 is multiplied by the imaginary number i and added to the equation for σ_1. Define $\Sigma = \sigma_1 + i\sigma_2$, and the differential equation for the complex coordinate Σ is:

$$\ddot{\Sigma} + \eta\dot{\Sigma} + p^2\Sigma = (B + iC)e^{-i\psi_1} + \frac{\gamma\mu}{6}(\sigma_0 + i\dot{\sigma}_0)e^{-i\psi_1} + \frac{\gamma\mu}{6}(\sigma_3 - i\dot{\sigma}_3)e^{i\psi_1} \quad (2)$$

Near hovering flight, the dynamic coupling between the coning motion (σ_0) and the Σ motion may be neglected. The coupling of σ_3 is through periodic coefficients and can also be neglected at low advance ratios.

Now to transfer to a stationary coordinate system

$$\delta = -\Sigma e^{i\psi_1} \quad (3)$$

where δ may be physically identified as the coordinate which describes the tilting of the tip-path-plane.

$$\delta = a_1 + ib_1$$

It is a complex form of the multiblade coordinates of Ref. 4 and is referred to as flapping in this paper.

A complex control displacement and a complex angular rate of rotation of the rotor are defined:

$$\Delta_c = A_1 + iB_1 \qquad \nu = q + ip$$

The differential equation for δ is

$$\ddot{\delta} + (\eta - 2i)\dot{\delta} + \eta(\alpha - i)\delta = \eta(\Delta_c - [1 - \frac{2}{\eta}i]\nu - \frac{1}{\eta}\dot{\nu} + m_z) \quad (4)$$

where $\alpha = (p^2 - 1)/\eta$.

The dimensionless aerodynamic moment applied to the rotor blades in steady flight is denoted by ηm_z. Note that the influence of angular rates, cyclic pitch and flapping are not contained in this term but are expressed separately.

The complex formulation has converted the two equations of motion describing the tilting of the tip-path-plane to a single second-order differential equation with complex coefficients given by Eq. (4). The complex coordinate δ is a normal coordinate at zero advance ratio. The coupling between δ and its conjugate may be neglected at low advance ratios.

Consider the nature of the transient solution to this differential equation. Note that the equation of motion has complex coefficients and therefore the roots of the characteristic equation will not in general be a complex conjugate pair. The physical interpretation of the roots is somewhat different from the case in which real coordinates are used.

Given a root of the characteristic equation $\sigma + i\omega$, the motion of δ corresponding to this root will be of the form $\delta = C_1 e^{(\sigma + i\omega)\tau}$.

Since δ is a complex number, the imaginary part of this root, ω, determines the rotation rate of the complex vector δ about the origin and σ determines its magnitude change with time. If ω is positive, this motion is counterclockwise rotation corresponding to an advancing mode, i.e., in the same direction as the rotor rotation. A negative ω corresponds to a regressing mode with respect to the frame of reference selected. Note that there is no simple correspondence between the sign of the imaginary term and the direction of rotation of a mode when real coordinates are used. If σ is equal to zero, then the vector δ describes a circle and a whirling mode is present. If σ is negative, the motion is a spiral which proceeds towards the origin.

Steady-State Response

First consider the nature of the steady-state response in hovering flight, that is, the flapping due to a constant control input or to a constant angular rate of rotation of the shaft, after the transient motion has subsided. Setting the acceleration and rate terms to zero, the following expression for the flapping is obtained:

$$\delta_{ss} = \frac{\Delta_c - (1 - \frac{2}{\eta}i)\nu + m_z}{\alpha - i} \tag{5}$$

The steady-state flapping produced by a control deflection will have its magnitude and phase changed by the flapping stiffness parameter α. As a function of α, the phase and amplitude of the flapping varies as shown in Fig. 1 for a real (A_1) unit control input. To determine the flapping for any other phase of control deflection, the diagram simply is rotated an appropriate amount. The flapping response to a constant angular velocity of the shaft is shown as a function of the stiffness parameter α for various Lock numbers in Fig. 2. The variation of flapping with stiffness describes a semicircle at a given Lock number. The flapping response produced by an angular velocity is rotated with respect to the response to control deflection and its magnitude is changed as a result of the difference in the phase and amplitude of the input. A rotor blade experiences both inertial and aerodynamic moments when the shaft has an angular velocity as expressed by the factor $(1 - (2/\eta)i)$ in Eq. (5).

It can be shown from the analysis of Ref. 9, that an approximate expression for the hub moment at low advance ratios consistent with the rotor blade model employed is given by

$$\frac{C_{mz_{ss}}}{a\sigma} = \frac{a\delta_{ss}}{16} \tag{6}$$

if a small term depending upon the angular rate of rotation of the shaft is neglected. A complex moment coefficient is defined as $C_{mz} = C_m + iC_l$. The steady-state hub moment produced by control deflection and pitch rate is also presented in Fig. 1 and 2 as a function of stiffness and Lock number. The phase angle of the hub moment response is the same function of α as the flapping as shown by the above expression. The variation of the hub moment with stiffness is a semicircle rotated 90° from the flapping response as a result of the dependence of the magnitude of the hub moment on the stiffness. These diagrams appear to present a clearer picture of the nature of the trends of rotor steady-state behavior with flapping stiffness changes and Lock number than is found for example in Ref. 9.

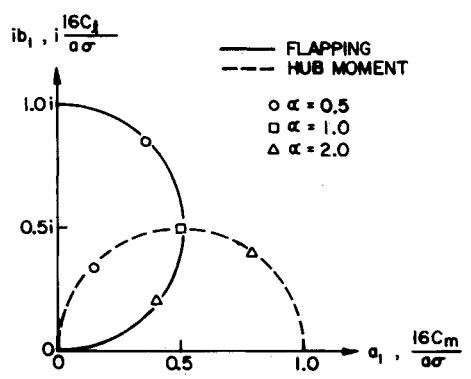

Fig. 1 Steady-state rotor characteristics. Flapping and hub moment variation with stiffness for a unit real control input (A_1).

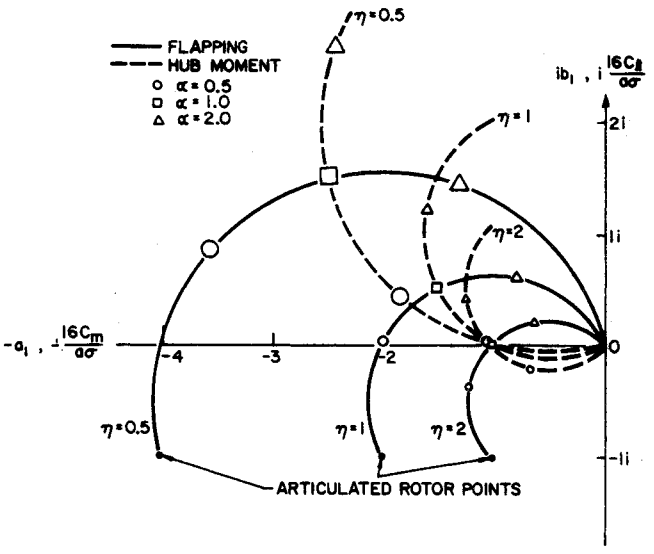

Figure 2 Steady-state rotor characteristics. Flapping and hub moment variation with stiffness and Lock number for a unit real angular velocity of the rotor shaft (q).

As a rotor is moved forward through the air, the blades will be acted upon by additional aerodynamic moments expressed by the term m_z. It may be seen from Eq. (5) that the effects of this moment in producing flapping will be altered in the same manner as flapping due to control deflection as the stiffness is varied. At low speeds, the lateral flapping of an articulated rotor is difficult to predict analytically owing to its dependence on the longitudinal induced velocity variations as shown by Harris.[10] However, Harris' data can be used directly to examine the behavior of a rotor with various levels of stiffness as a function of advance ratio.

If there is a complex aerodynamic moment m_z acting on the rotor blades, then the steady-state flapping response $\delta_{ss} = m_z/(\alpha - i)$. Thus, the flapping of an articulated rotor ($\alpha = 0$) can be interpreted as arising from an aerodynamic input (m_z) rotated 90° clockwise from the flapping, as shown in Fig. 3. Also note that the hub moment produced by an infinitely rigid rotor ($\alpha \to \infty$) is $16C_{mz}/a\sigma = m_z$.

As the stiffness of the rotor is varied between these two limits, the flapping and the hub moment produced by the rotor will vary as shown on the diagram. The figure shows the hub moments which must be balanced by cyclic control as a function of stiffness and advance ratio. As stiffness increases, the rotor response tends to become less coupled in the sense that the rolling moment due to forward speed is reduced. It is interesting to note from the Eqs. (5) and (6) that if there is no fuselage moment or center of gravity offset to be trimmed, then the cyclic control required to balance the hub moments is independent of stiffness ($\Delta_c = m_z$) since $\delta_{ss} = 0$. Similarly it may be noted that the steady-state rate developed by a rotor as a result of a control input in hovering is independent of

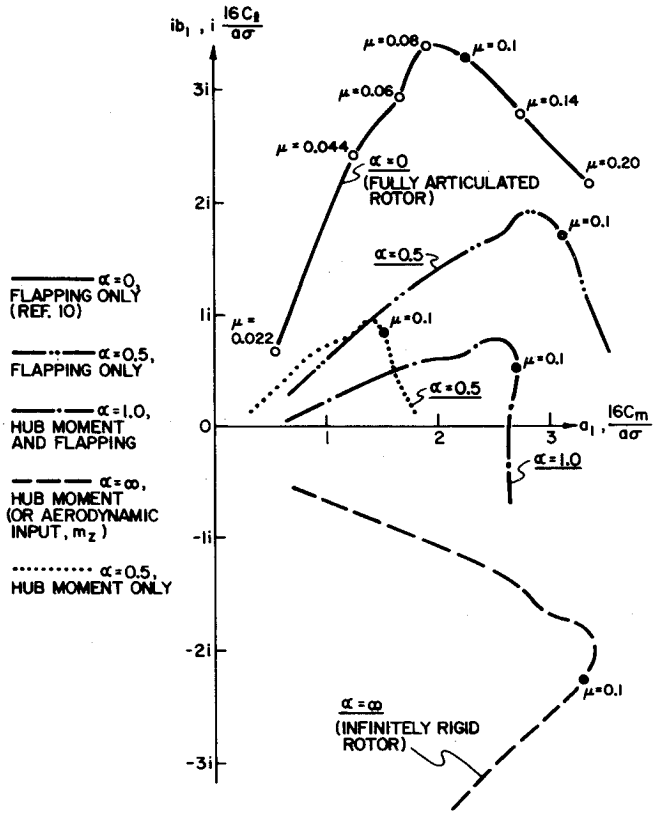

Fig. 3 Steady-state rotor characteristics. Flapping and hub moment variation with forward speed as a function of stiffness.

stiffness if the control input phasing is not changed from the fully articulated rotor setting as stiffness is increased. The control normally would be rephased to produce pure rolling and pitching acceleration as a result of an initial input. Consequently, the ratio of pitch rate to roll rate would change with stiffness, due only however to control phasing as noted in Ref. 8. This phase alteration would also result in a change in the stick motion required to trim as a function of forward speed as stiffness is varied although the net cyclic pitch amplitude to trim is independent of stiffness.

Inflow Considerations

It has been shown[8,11] that in the prediction of hingeless rotor characteristics it is important to consider first harmonic inflow variations produced as a result of the development of an aerodynamic hub moment by the rotor. The nature of this effect on rotor flapping and hub moments can be developed quite simply using complex notation. A first harmonic inflow variation is added to the flapping equation and will not appear directly in the hub moment equation owing to the rotor blade model used. The harmonic inflow is assumed for simplicity to be independent of radius.[11] Other assumptions regarding the variation of inflow with radius will not change the essential results of this analysis. The steady-state form of Eq. (4) in hovering, modified to account for inflow variations is:

$$(\alpha - i)\delta_{ss} = \Delta_c - (1 - \frac{2}{\eta}i)\nu - \frac{4}{3}\Delta\lambda \qquad (7)$$

where

$$\Delta\lambda = \lambda_c + i\lambda_s$$

The expression for the hub moment is given by Eq. (6). The hub moment is expressed in terms of the elastic moment at the root of the blade which is equal to the aerodynamic moment at the root plus the direct inertial moment due to angular velocity ν. It is assumed that the harmonic inflow is proportional only to the aerodynamic moment at the root. Rearranging Eq. (7):

$$\alpha\delta_{ss} = i\delta_{ss} + \Delta_c - \frac{4}{3}\Delta\lambda - \nu + i\frac{2}{\eta}\nu \qquad (7a)$$

The last term in this equation can be identified as a direct inertial moment acting on the rotor blades. Therefore, the inflow change is proportional to the first four terms on the right-hand side of Eq. (7a)

$$\Delta\lambda = j(\frac{16\,C_{mz}}{a\sigma})_{\text{aero}} = j(i\delta_{ss} + \Delta_c - \nu - \frac{4}{3}\Delta\lambda) \qquad (8)$$

Substituting this relationship into the flapping equation gives

$$(\alpha^* - i)\delta_{ss} = \Delta_c - (1 - (2/\eta^*)i)\nu \qquad (9)$$

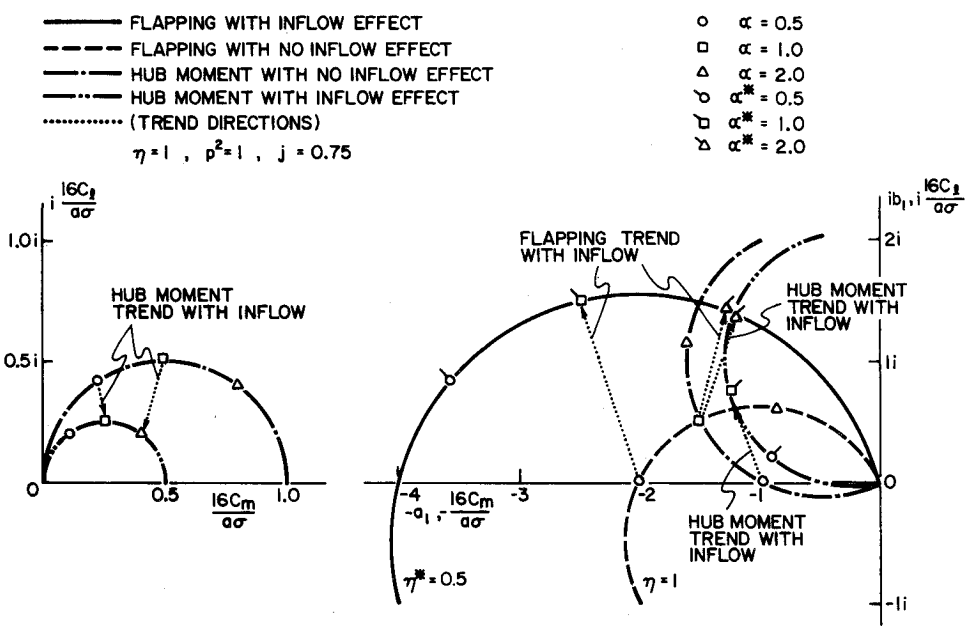

Fig. 4 Steady-state rotor characteristics. First harmonic inflow effects on flapping and hub moment due to control deflection and angular velocity.

where

$$\alpha^* = (1 + (4/3)j)\alpha \qquad \eta^* = \frac{\eta}{1 + (4/3)j}$$

This modification to the flapping equation can be interpreted as a change in Lock number.[8] Note that the parameter α appearing in Eq. (6) is not changed.

The factor j may be selected based on a variety of theoretical models as indicated in Ref. 11. A real value of j represents a direct proportionality between the hub moments and the inflow. A complex value of j would represent a phase shift between the hub moment and the inflow. More complex inflow models such as found in Ref. 11 would require introducing the conjugate of $\Delta\lambda$, however, if only the hovering case is considered, symmetry considerations rule out more elaborate models. Therefore, rearranging Eq. (9)

$$\delta_{ss} = \frac{\Delta_c}{\alpha^* - i} - \frac{[1 - (2/\eta^*)i]}{(\alpha^* - i)}\nu \qquad (9a)$$

The inflow effect produces an amplitude change and a phase shift in the flapping response to a control input which can be directly determined from Fig. 1 by using α^* in place of α. The angular velocity response would be modified in two ways. The effect of the inflow would be to change η as well as α. Note that the flapping due to an angular velocity is increased by this effect and that the damping of a fully articulated rotor is therefore altered by harmonic inflow.

The hub moment per unit control deflection is

$$\frac{1}{\Delta_c}\frac{16C_{m_\beta}}{a\sigma} = \frac{1}{1 + (4/3)j}\left(\frac{\alpha^*}{\alpha^* - i}\right) \qquad (10)$$

Thus the phase and the amplitude of the hub moment due to control deflection are changed. The amplitude of the hub moment is reduced by the factor:

$$\frac{1}{1 + (4/3)j}$$

The hub moment due to angular velocity is also reduced by the same factor

$$\frac{1}{\nu}\frac{16C_{m_\beta}}{a\sigma} = \frac{1}{1 + (4/3)j}\left(\frac{-\alpha^*(1 - (2/\eta^*)i)}{\alpha^* - i}\right) \qquad (11)$$

from that expected based only on the changes in α^* and η^*. The influence of these inflow effects on the results presented in Figs. 1 and 2 are shown in Fig. 4 for a value of j = 3/4. This value is predicted by momentum theory for a typical hovering rotor.[11]

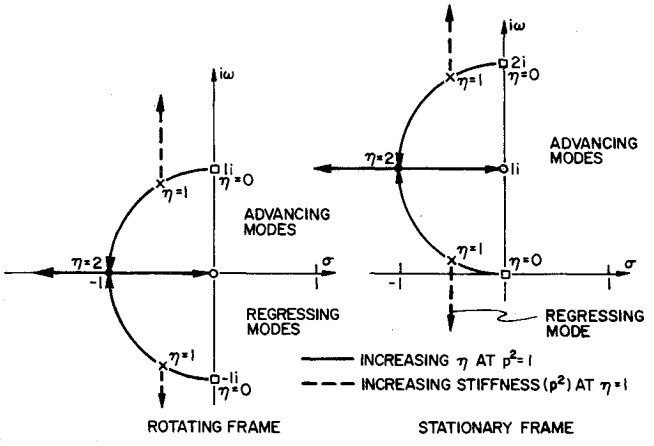

Fig. 5 Tip-path-plane modes of motion as a function of Lock number and stiffness.

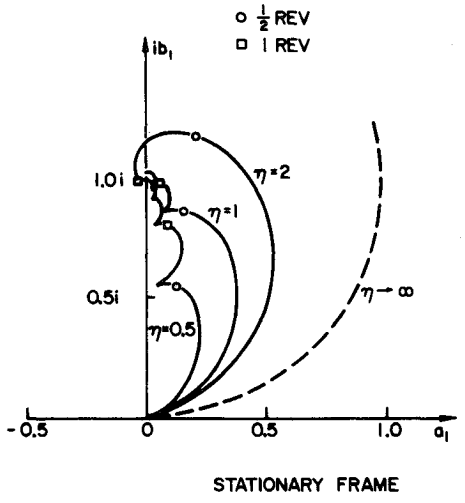

Fig. 6 Transient response of tip-path-plane for unit real control step input.

These results show the importance of the first harmonic inflow on rotor characteristics particularly as rotor stiffness is increased.

Transient Response

The transient response of the tip-path-plane to inputs may be readily calculated from Eq. (4) since it is of second-order.

The characteristic roots are shown as a function of the parameter η in Fig. 5 in the rotating and stationary coordinate systems. In the rotating coordinate system, a symmetric pattern corresponding to an advancing mode and a regressing mode results. In the stationary coordinate system, these two modes are both advancing modes, one is rapid and the other is slow. As flapping stiffness is increased from zero, the slowly advancing mode becomes a regressing mode as shown in Fig. 5.

Consider the transient response of the rotor plane to a step input in control. Only a real control is considered, and any other phase control input will rotate the resulting response diagram. Transient responses are shown for a fully articulated rotor in Fig. 6, as a function of Lock number. This graph may be viewed as a picture of the tilting tip-path-plane of the rotor as it moves towards equilibrium. It is interesting to note that as the Lock number is increased, there is considerably more longitudinal tilting of the tip-path-plane due to a lateral input (A_1) as well as overshoot owing to the fact that the Lock number affects the size of the disturbance as well as the damping ratio (in a rotating frame). However, the rotor plane is much closer to its steady-state condition in one revolution of the rotor as Lock number is increased as shown on the diagram. From the viewpoint of the stationary reference frame, the amplitude increase arises in part from the fact that the two modes of motion come closer together as the Lock number is increased, eventually becoming equal when the Lock number is equal to 16.

The velocity of the tip-path-plane is not constant along these curves. The cusps on the curves are points at which the velocity of the tip-path-plane is momentarily equal to zero.

In the limit of very large η, the tip-path-plane executes a circle about the steady-state value and in the limit η = 0 there is no motion. For comparison with the stationary frame results, the response of the tip-path-plane in a rotating frame of reference is shown in Fig. 7. The arrows show the direction of motion with time.

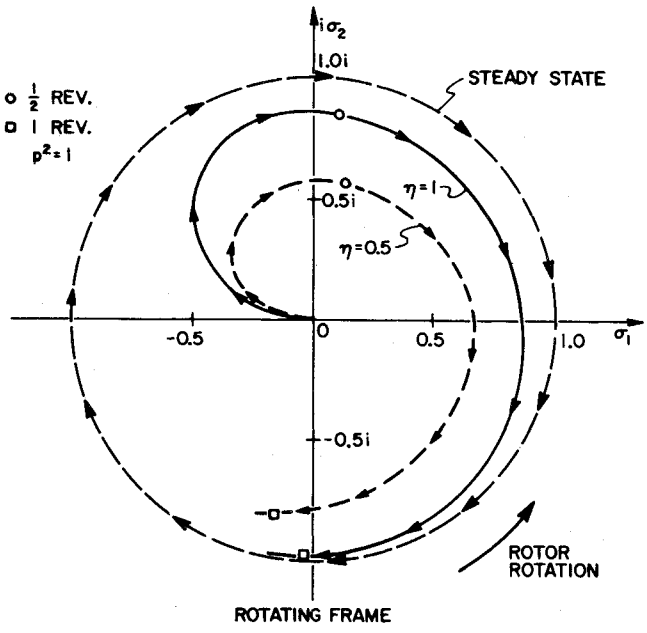

Fig. 7 Transient response of tip-path-plane for unit real control step input.

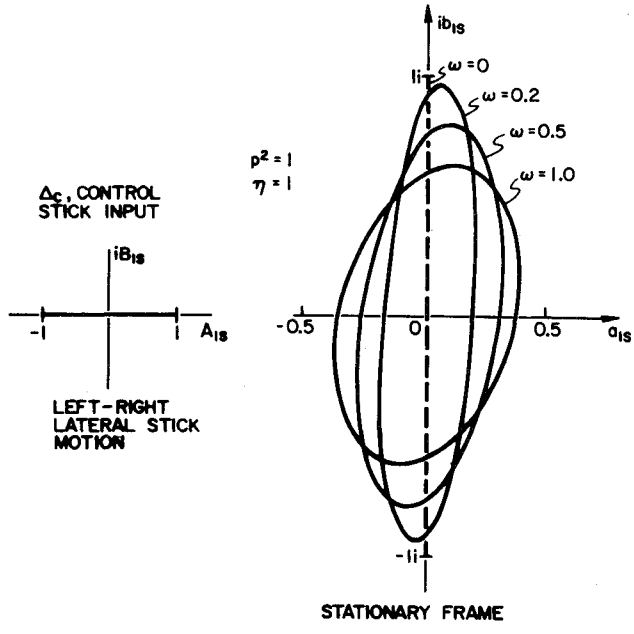

Fig. 9 Frequency response of tip-path-plane for unit control input. Linear motion of control.

Frequency Response

The response of the rotor tip-path-plane to sinusoidal inputs can also be readily calculated. Denote the transfer function $\delta/\Delta_c = A(s)$. Consider first a complex control input of the form $\Delta_c = e^{i\omega\tau}$. This input to the rotor plane is physically a constant unit amplitude rotation of the control stick in a circle in the same direction as the rotor rotation. The amplitude and phase of the sinusoidal response of the tip-path-plane produced by this input shown in Fig. 8 for various Lock numbers at positive and negative input frequencies. The steady-state motion of the tip-path-plane is a circle with an amplitude and phase relationship relative to the control amplitude and phase given by the frequency response characteristic $[A(i\omega)]$. The response differs for positive and negative input frequencies in the stationary reference frame. That is, a rotation of the control stick in the direction of rotor rotation results in a different amplitude and phase characteristic from rotation opposite to the direction of rotation owing to the complex coefficients in the transfer function. Again note that the amplitude of the response increased with increasing Lock number, although the damping ratio of the system when viewed in the rotating coordinate system is increasing.

Now if the control stick is oscillated in a straight line, the control motion is represented by a linear combination of a positive frequency of rotation and a negative frequency of rotation of equal amplitude

$$\Delta_c = \frac{e^{i\omega\tau} + e^{-i\omega\tau}}{2} \tag{11}$$

and the resulting steady-state response is

$$\delta = \frac{1}{2}A(i\omega)e^{i\omega\tau} + \frac{1}{2}A(-i\omega)e^{-i\omega\tau} \tag{12}$$

It may be shown that this result corresponds to an elliptical motion of the tip-path-plane. The major axis of the ellipse is equal to $(|A[i\omega]| + |A[-i\omega]|)$ and the minor axis equal to $(A[i\omega]| - |A[-i\omega]|)$. The major axis is located at an angle equal to ½ (arg $A[-i\omega]$ + arg $A[-i\omega]$) from the real axis for a real control input. The tip-path-plane motion is shown in Fig. 9 as a function of input frequency for a straight line control oscillation. Linear motion of the control at any combination of lateral and longitudinal cyclic will rotate the ellipse. The tip-path-plane motion around the ellipse is in the direction of rotor rotation as indicated by the larger magnitude of the response at positive frequencies shown in Fig. 8.

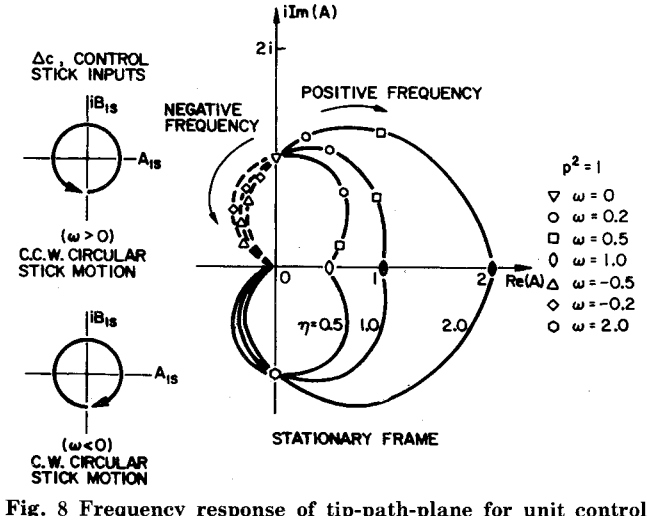

Fig. 8 Frequency response of tip-path-plane for unit control input. Angular rotation of control.

Flapping Feedback

There has been extensive discussion of various flapping feedbacks in the literature[1-4] to provide a means for reducing the gust sensitivity of hingeless rotors. While much of the interest centers around achieving improved behavior at high speeds, the complex formulation described here provides an ideal framework in which to study the influence of these feedbacks on the response of the rotor plane and to show their primary features in terms of hovering and low speed behavior. The complex formulation makes possible direct use of root locus techniques to study flapping feedbacks.

It should be noted here that all flapping feedback is assumed to take place through the mechanism of a swash plate. In any mechanical feedback system such as Oemichen linkage where the pitch angle of one blade is linked

directly to the flap angle of another blade, the effects of this feedback will be felt in other modes of motion, i.e., other combinations of the individual blade flapping angles and the complete picture is not given by considering only the tip-path-plane tilting dynamics.

Consider a tilt proportional feedback. This may be expressed in complex notation as

$$\Delta_c = K_P(ie^{i\epsilon})\delta \tag{13}$$

where K_P and ϵ may be selected as desired. With $\epsilon = 0$ this feedback corresponds to the physically logical feedback of moving the swash plate in such a way as to reduce the flapping amplitude. Choosing $\epsilon = 180°$ would be equivalent to changing the sign of the gain and would be expected to lead to divergent tip-path motion as the gain is increased.

Various particular values of ϵ correspond to well-known systems as follows: $\epsilon = 90°$ corresponds to a negative δ_3 hinge (pitch decreases with upward flapping); $\epsilon = 270°$ corresponds to a positive δ_3 hinge (pitch increases with flapping); $\epsilon = 0$ corresponds to an Oemichen hinge, with the restriction that only cyclic pitch through a swash plate is employed in the feedback and that a four-bladed rotor is considered. The influence of an Oemichen hinge on the tip-path-plane motion of a rotor with b blades is determined by selecting $\epsilon = 2\pi/b - \pi/2$. No coning effects are included.

Placing the feedback law in the characteristic equation and arranging the characteristic equation in root locus form:

$$\frac{(K_P ie^{i\epsilon})\eta}{s^2 + (\eta - 2i)s + \eta(\alpha - i)} = 1 \tag{14}$$

The root locus method can be generalized to include angle conditions other than zero and 180° (ϵ other than 90° or 270°) and the variations of the roots with gain K_P at various ϵ can be conveniently sketched. Again recall that because of the complex coefficients, the root loci will no longer be symmetric about the real axis. Conventional root locus rules must be extended to account properly for the phase requirement on the denominator of the above expression, which is no longer restricted to 0 or 180° for arbitrary ϵ. The effects of various feedback phase angles and gains on the tilting modes of motion of the tip-path-plane are shown in Fig. 10.

This root locus indicates a low gain stability limit for $\epsilon = 0$ with the fast advancing mode showing an oscillatory instability as the gain is increased. The locus shows the

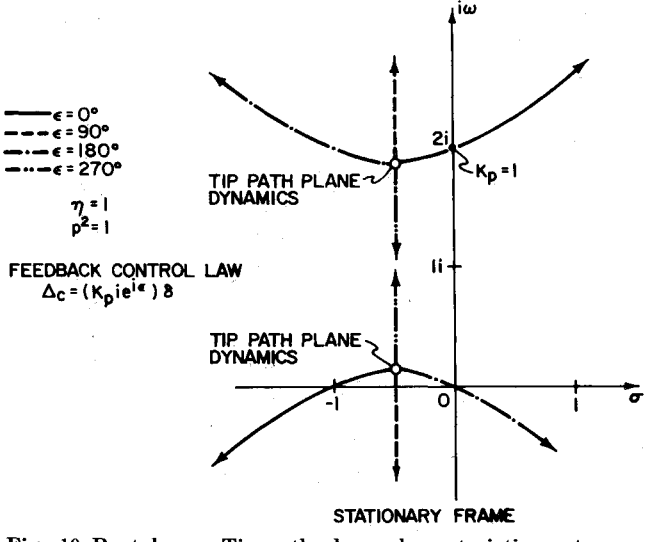

Fig. 10 Root locus. Tip-path-plane characteristic roots as a function of gain and phase for proportional feedback.

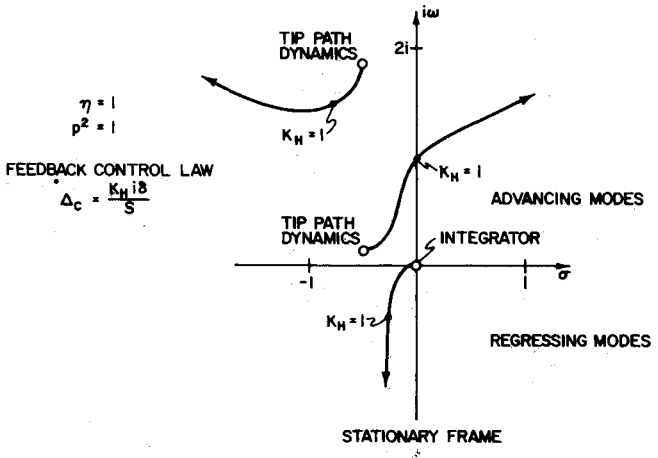

Fig. 11 Root locus. Tip-path-plane characteristic roots as a function of gain for integral feedback.

difficulty in achieving flapping amplitude reductions by proportional feedback. The amplitude of the response to a constant disturbance in the stationary frame is proportional to the reciprocal of the distance of the low frequency root from the origin, assuming that the distance to the high frequency root is not changed appreciably as the gain and phase are varied. The best compromise between stability and reduction in response amplitude appears to be achieved with ϵ somewhere between 0 and 90°.

Various kinds of integral feedback have also been proposed to improve the low frequency response characteristics of a hingeless rotor. These can be readily examined. Consider an integral feedback as proposed by Hohenemser[4]

$$\Delta_c = \frac{K_H i\delta}{s} \tag{15}$$

Again a root locus can be sketched for this feedback system. In this case, the angle criterion to be applied for positive gain is 90° and results in the root locus shown in Fig. 11. The slowly advancing mode becomes unstable as the gain is increased.

Conclusions

Transformation of the coordinates describing the tilting of the tip-path-plane of a rotor to complex form results in a convenient approach to the study of rotor tip-path-plane dynamics at low advance ratios. The order of the dynamic system is reduced from four to two by this transformation. The transient response and the frequency response of the tilting of the tip-path-plane can be simply calculated and readily visualized as a function of various rotor parameters and the flight condition.

An extension of the root locus method has been presented which is particularly useful in the study of flapping feedback and its influence on the dynamics of the tip-path-plane.

References

[1]Hohenemser, K. H. and Johnson, R. L., "On the Dynamics of Lifting Rotors with Thrust or Tilting Moment Feedback Controls," *Journal of the American Helicopter Society*, Vol. 15, No. 1, Jan. 1970, pp. 42–54.

[2]Sissingh, G. J., "Dynamics of Rotors Operating at High Advance Ratios," *Journal of the American Helicopter Society*, Vol. 13, No. 3, July 1968, pp. 56–63.

[3]Hohenemser, K. H. and Peters, D. A., "Application of the Floquet Transition Matrix to Problems of Lifting Rotor Stability," *Journal of American Helicopter Society*, Vol. 15, No. 2, April 1971, pp. 25–33.

[4]Hohenemser, K. H. and Yin, Shen-Kuang, "Some Applications of the Method of Multi-blade Coordinates," *Journals of the American Helicopter Society*, Vol. 17, No. 3, July 1972, pp. 3–12.

[5]Coleman, R. P., "Theory of Self-Excited Mechanical Oscillations of Hinged Rotor Blades," NACA Advanced Restricted Rept. 3G29, Republished as Rept. 1351, 1943, NACA.

[6]Miller, R. H., "Helicopter Control and Stability in Hovering Flight," *Journal of the Aeronautical Sciences*, Vol. 15, No. 8, Aug. 1948, pp. 453–472.

[7]Azuma, A., "Dynamic Analysis of the Rigid Rotor System," *Journal of Aircraft*, Vol. 4, No. 3, May-June 1967, pp. 203–209.

[8]Curtiss, H. C., Jr. and Shupe, N. K., "A Stability and Control Theory for Hingeless Rotors," American Helicopter 27th Annual National V/STOL Forum, Washington, D. C., May 1971.

[9]Ward, J. F., "Exploratory Flight Investigation and Analysis of Structural Loads Encountered By A Helicopter Hingeless Rotor System," D-3676, Nov. 1966, NASA.

[10]Harris, F. D., "Articulated Rotor Blade Flapping Motion at Low Advance Ration," *Journal of the American Helicopter Society*, Vol. 17, No. 1, Jan. 1972, pp. 41–48.

[11]Ormiston, R. A. and Peters, D. A., "Hingeless Helicopter Rotor Response with Nonuniform Inflow and Elastic Blade Bending," *Journal of Aircraft*, Vol. 9, No. 10, Oct. 1972, pp. 730–736.

MAY 1973 J. AIRCRAFT VOL. 10, NO. 5

Vortex Noise of Isolated Airfoils

Robert W. Paterson,* Paul G. Vogt,† Martin R. Fink‡
United Aircraft Research Laboratories, East Hartford, Conn.
and
C. Lee Munch§
Sikorsky Aircraft Division, Stratford, Conn.

An experimental study of airfoil vortex shedding noise in a low-turbulence flow and in a Reynolds number range applicable to full-scale helicopter rotors is described. Measurements of far-field noise, airfoil surface pressure fluctuations and correlation coefficients were obtained for NACA 0012 and NACA 0018 two-dimensional models and a finite-span NACA 0012 airfoil. Airfoil vortex shedding noise was found to be discrete rather than broadband, with the frequency predicted by a Strouhal number of approximately 0.1 referenced to twice the trailing-edge laminar boundary-layer thickness. At Reynolds numbers and angles of attack for which this boundary layer was turbulent on both surfaces, vortex shedding noise was undetectable. The effects of airfoil thickness change and finite airfoil span were found to be small, consistent with their influence on the pressure-surface laminar boundary layer. Cited examples of helicopter tail rotor, model propeller, sailplane flyby and low-Reynolds number isolated-airfoil data show that vortex shedding noise exists on these devices as a discrete-frequency phenomenon with the frequencies well predicted by the scaling law developed in the present study.

Introduction

HELICOPTER rotor and propeller noise spectra exhibit both a discrete-frequency and broadband character. The discrete-frequency or rotational noise is caused by steady and periodically fluctuating blade loads at frequencies which are integer multiples of blade rotative speed. The sources of broadband noise can be conveniently grouped into those present when a stationary, isolated airfoil is immersed in a uniform stream and those associated with blade rotation and inter-blade effects. The potentially important sources of noise for an isolated airfoil are; 1) vortex shedding, 2) incident turbulence, 3) the turbulent boundary layer, and 4) wake generated noise.

Vortex shedding is caused by interaction of the airfoil's wake-induced velocity field with the airfoil itself. The classic example of this mechanism is the Karman vortex street which occurs in a highly organized fashion in the wake of bluff bodies. The second noise mechanism[1,2] arises from random fluctuations in the turbulent velocity components incident on the airfoil which cause effective angle-of-attack changes, unsteady loads and hence noise. The third source is the turbulent boundary layer[3] which radiates noise directly and also produces edge noise, a mechanism arising from convection of turbulence past the sharp trailing edge. The fourth source is direct radiation from the turbulent wake.

Discrete frequency vortex shedding noise of vanes in water was clearly identified by Gongwer[4] who also related the frequency to a Strouhal number referenced to the sum of blunt trailing edge and turbulent boundary-layer thicknesses. Another study, however, found the relevant Strouhal number length scale for shedding to be the airfoil projection normal to the stream.[5] Sharland[1] conducted mea-

Presented as Paper 72-656 at the AIAA 5th Fluid and Plasma Dynamics Conference, Boston, Mass., June 26–28, 1972; submitted July 5, 1972; revision received February 21, 1973. The experimental study reported herein was funded by the Army Research Office, Durham, under Contract DAHCO4-69-C-0089. The authors wish to acknowledge the efforts of G. W. Johnston (presently of University of Toronto, Institute of Aerospace Sciences) and R. G. Schlegal (Sikorsky Aircraft) for their efforts in the initiation of the present study. Discussions with the latter and A. A. Peracchio and R. K. Amiet (UARL) during the course of the study were most helpful.

Index categories: Aerodynamic and Powerplant Noise (Including Sonic Boom); Aircraft Propulsion System Noise; Nonsteady Aerodynamics.

*Research Engineer, Aeroacoustics Group.

†Research Engineer, Aeroacoustics Group. Associate Member AIAA.

‡Senior Consulting Engineer, Aerodynamics. Associate Fellow AIAA.

§Acoustics Engineer.